Elastocapillary powered manipulation of liquid plug in microchannels

D. George, R. Anoop, and A. K. Sen

Citation: Appl. Phys. Lett. **107**, 261601 (2015); doi: 10.1063/1.4939116
View online: http://dx.doi.org/10.1063/1.4939116
View Table of Contents: http://aip.scitation.org/toc/apl/107/26
Published by the American Institute of Physics

Elastocapillary powered manipulation of liquid plug in microchannels

D. George, R. Anoop, and A. K. Sen
Department of Mechanical Engineering, Indian Institute of Technology Madras, Chennai 600036, India

(Received 13 October 2015; accepted 15 December 2015; published online 30 December 2015)

We report the manipulation of a liquid plug inside a rectangular microchannel, when one of the channel walls is a deformable membrane, which adjoins another parallel microchannel. Elastocapillary flow of a driving liquid (DL) through the adjoining microchannel, when approaches the plug, tries to pull the membrane near the plug, which is initially deflected into the plug, towards the DL. The plug is transported due to a differential pressure that develops across the plug owing to the increase in the radius of curvature of the trailing meniscus of the plug. A theoretical model is proposed to predict the plug velocity, which depends on a parameter J and plug length $\tilde{L}$. The predictions of the theoretical model show good agreement with experimental data. The dynamic behaviour of the plug and DL is presented and discussed. © *2015 AIP Publishing LLC*.
[http://dx.doi.org/10.1063/1.4939116]

Rapid development of microfluidics is ascribed to its myriads of applications in miniaturized bio-analysis, point of care diagnosis, and drug delivery.[1] Owing to this interest, studies on capillary flows[2] have seen a renaissance in the last decade.[3–6] Subsequently, characteristics of capillary flows were exploited to develop complex self-powered microfluidic systems.[7–9] Studies on the possible use of capillarity and elasticity for mass production of 3D micro and nanoscale objects—capillary origami—are also reported.[10] In elastocapillary flow through deformable micro and nanochannels, significant enhancements in capillary flow performance have been observed.[11,12] Dynamic and static analyses of elastocapillary phenomena have also been reported.[13,14] Dynamics of liquid plugs in narrow confinements received attention mainly due to its significance in pulmonary system[15] and oscillating heat pipes.[16] In nature, certain sea birds utilize the pressure difference across the two menisci of capillary plugs for the transport of prey-laden water droplets mouthward.[17] Self-propagation of liquid plugs in narrow channels was achieved in a tapered capillary tube[18] and by juxtaposing two liquid plugs of different surface tension values.[19] However, the applications of later techniques in microfluidics may be limited by the fabrication complexity, lack of proper control over the plug once it is placed inside a microchannel, or the adulteration of the liquid plug due to the use of additional liquids.

Here, we report the transport of a liquid plug inside a rectangular microchannel, when one of its walls is a deformable membrane, which adjoins another parallel microchannel (Fig. 1). Due to the Laplace pressure jump across its curved interfaces, the liquid plug is below ambient pressure.[20] The bottom membrane wall of the microchannel containing the plug deflects into the plug due to the difference in pressure between the plug and the ambient air inside the adjoining microchannel. A driving liquid (DL) is introduced at the inlet of the adjoining microchannel, which fills the channel due to capillary action. When the DL approaches the plug, the membrane near plug is pulled downward into the DL thus increasing the radius of curvature of the trailing interface of the plug. A differential pressure is created across the plug due to which it is transported in the direction of the DL flow. We report a theoretical model to predict the plug velocity, which depends on a non-dimensional parameter J and plug length $\tilde{L}$. The location of the leading end of the plug and DL menisci with time and the effects of membrane thickness and plug length on the plug velocity are predicted using model and experimentally measured. Finally, the important flow regimes are identified and discussed.

First, we analyse the initial upward deflection of the membrane due to the pressure difference $-p_p(x)$ between the plug and ambient air inside the adjoining microchannel (Fig. 1(a)). Consider a thin rectangular membrane of width w, length L, and thickness t with its edges $y = \pm w/2$ built-in. Let E and ν denote, respectively, its Young's modulus and Poisson's ratio. Assuming the pure bending theory for thin plates gives a reasonable approximation (since maximum deflection is less than half the membrane thickness), we take $\frac{\partial^4\omega}{\partial x^4} + 2\frac{\partial^4\omega}{\partial x^2\partial y^2} + \frac{\partial^4\omega}{\partial y^4} = -\frac{p_p(x)}{D}$, where $D = Et^3/12(1-\nu^2)$ is the flexural rigidity. By using $x' = x/L$, $y' = y/w$, $\omega' = \omega/\hat{\delta}_p$, and $p'_p(x') = p_p(x)w^4/\hat{\delta}_p D$, where $\hat{\delta}_p$ is maximum membrane deflection, we obtain the non-dimensional equation (primes dropped for clarity)

$$\varepsilon^4\frac{\partial^4\omega}{\partial x^4} + 2\varepsilon^2\frac{\partial^4\omega}{\partial x^2\partial y^2} + \frac{\partial^4\omega}{\partial y^4} = -p_p(x). \tag{1}$$

Since $\varepsilon = w/L \ll 1$, the terms involving ε^4 and ε^2 are being neglected. Now, integrating the simplified equation, using boundary conditions at the built-in edges; $\omega = 0$ at $y = \pm\omega/2$ and $d\omega/dy = 0$ at $y = \pm w/2$, we get

$$\omega(x,y) = \delta_p(x)\left(4\left(\frac{y}{w}\right)^2 - 1\right)^2, \tag{2}$$

where $\delta_p(x) = \omega(x,0) = -\alpha p_p(x)w^4/D$ is the maximum deflection, at any given x, which occurs at $y = 0$, the constant $\alpha = 1/384$. The pressure $-p_p(x)$ acting on the membrane is maximum and thus the maximum deflection $\hat{\delta}_p$ occurs at $x = \hat{x}_p$, a short distance away from the plug

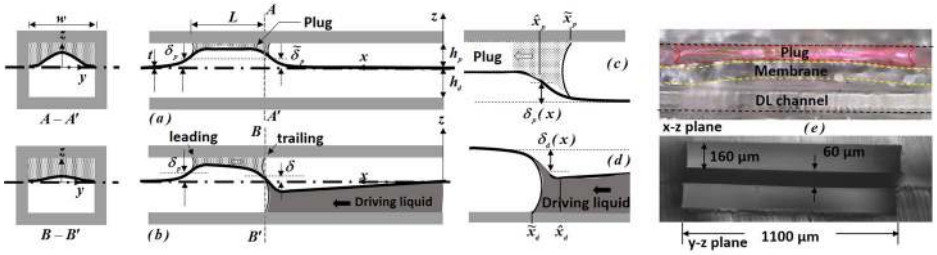

FIG. 1. (a) Liquid plug (indicated by dotted area) and the resulting membrane deflection. (b) DL approaches the trailing interface of the plug thus pulls membrane downward and changes the curvature of the trailing interface. Close-up views of the (c) plug meniscus and (d) DL meniscus. (e) Optical images of the device.

meniscus $x = \tilde{x}_p$ (Fig. 1(c)). Our numerical simulations showed that $\tilde{\delta}_p = \hat{\delta}_p/2$ is a very good approximation, which is in agreement with the earlier works.[11] The change in pressure over the short distance from $\tilde{x}$ to $\hat{x}$ is neglected, so that $p_p(\tilde{x}_p) = p_p(\hat{x}_p) = -p_{mp}$. Assuming $w \gg h_p$, where h_p is the height of the plug channel, we equate the pressure jump across the plug meniscus p_{mp} with the pressure that corresponds to the membrane deflection $-p_p(x)$ as

$$2\sigma_p \cos\theta_p \left(\frac{1}{h_p - \delta_p}\right) = \frac{2\delta_p D}{\alpha w^4}, \tag{3}$$

where σ_p is the surface tension and θ_p is the contact angle of the plug. Solving for the upward deflection at the meniscus gives $\tilde{\delta}_p/h_p = \eta_p = (1/2)(1 - \sqrt{1 - J})$ where $J = 4\alpha w^4 \sigma_p \cos\theta_p / D h_p^2$, which represents the ratio of the capillary force to the mechanical restoring force. Initially, the radius of curvatures of the leading and trailing menisci of the plug and deflections of the membrane at these two locations are equal (i.e., $\tilde{\delta}_p$) (Fig. 1(a)).

When the DL is introduced, there is a downward deflection of the membrane close to the advancing capillary meniscus. When the meniscus of the DL approaches the trailing interface of the plug, it tends to pull the membrane downward. Since, at the trailing interface of the plug, the membrane is already deflected upward, the magnitude of this upward deflection is reduced (Fig. 1(b)). The resultant deflection of the membrane δ is obtained by considering the pre-existing upward pull owing to the pressure $-p_p(x)$ due to pressure jump across the trailing end of the plug and the competing downward pull owing to pressure $-p_d(x)$ due to the pressure jump across the DL meniscus as

$$\frac{2\eta D h_p}{\alpha w^4} = \frac{2\sigma_p \cos\theta_p}{h_p(1-\eta)} - \frac{2\sigma_d \cos\theta_d}{h_d\left(1 + \frac{h_p}{h_d}\eta\right)}, \tag{4}$$

where p and d denote plug and DL, respectively, and $\delta = h_p \eta$. The downward pull of the membrane near the trailing meniscus of the plug creates a difference in the radii of curvatures of the leading and trailing menisci of the plug. Thus, a differential pressure is created, which is responsible for the transport of the plug. When the plug is set to motion, there is a balance between the driving differential pressure $\Delta p_d = (\Delta p_l - \Delta p_t)$, i.e., difference between the pressure jumps at the leading and trailing menisci, $\Delta P_l = 2\sigma \cos\theta_{pl}/(h_p - \delta_p)$ and $\Delta P_t = 2\sigma \cos\theta_{pt}/(h_p - \delta)$, respectively, and the viscous pressure drop ΔP_v.[16,19] During experiments, we observed that the trailing meniscus of the plug completely wets the channel wall; thus, the dynamic contact angle of the trailing meniscus $\theta_{pt} \sim 0°$. The dynamic contact angle of the leading meniscus θ_{pl} is found in terms of the static contact angle θ_p using the expression[21] $\cos(\theta_{pl}) = \cos(\theta_p) - 2(1 + \cos(\theta_p))Ca^{0.5}$, where $Ca = (\mu_p U_p)/\sigma_p$, where μ_p is the plug viscosity and U_p is the plug velocity.

The viscous pressure drop ΔP_v is found by considering fully developed velocity profile $\mathbf{v}_p = u_p(y,z)\mathbf{e}_x$ and pressure $p_p(x)$ constant at a cross-section and using Poiseuille equation $\mu_p \nabla^2 u_p = \partial p_p/\partial x$ (similar to Ma[16] and Bico and Quéré[19]). By changing variables using $\bar{y} = y/w$, $\bar{z} = z/h_p$ and $\bar{u} = u_p/U_p$ (considering flow rate $Q_p = w h_p U_p$), we get

$$a_p^2 \frac{\partial^2 \bar{u}_p}{\partial \bar{y}^2} + \frac{\partial^2 \bar{u}_p}{\partial \bar{z}^2} = \frac{w h_p^3}{\mu_p Q_p}\frac{\partial p_p}{\partial x} = K_p, \tag{5}$$

where $a_p = h_p/w$ is channel aspect ratio and K_p is a constant. For channels of small aspect ratios (i.e., $h_p \ll w$), considered in our experiments, the first term in Equation (5) is dropped. Equation (2) gives the variation of the channel height across the width as $\bar{h}(\bar{y}) = 1 - \eta(4\bar{y}^2 - 1)^2$, where $\bar{h}(\bar{y}) = h(y)/h_p$ and $\eta = \delta_p(x)/h_p$. Using no-slip boundary conditions at the bottom $\bar{z} = 0$ and top $\bar{z} = h(\bar{y})$ walls, integrating Equation (5), we get the velocity profile $\bar{u}_p(\bar{y},\bar{z}) = (1/2)K_p \bar{z}[\bar{z} - \bar{h}(\bar{y})]$. The form of the non-dimensionalization requires $\int\int d\bar{y}\, d\bar{z}\, \bar{u}(\bar{y},\bar{z}) = 1$, from which we obtain $K_p = \frac{w h_p^3}{\mu_p Q_p}\left(\frac{\partial p_p}{\partial x}\right) = -12/F(\eta_p)$. So the hydraulic resistance per unit length $r_p = \frac{1}{Q_p}\left(-\frac{\partial p_p}{\partial x}\right) = \frac{12\mu_p}{\beta w h_p^3}\frac{1}{F(\eta_p)}$, where $F(\eta_p) = 1 - \frac{8\eta_p}{5} + \frac{128\eta_p^2}{105} - \frac{1024\eta_p^3}{3003}$. Thus, the average channel height $\bar{h}_p \approx h_p[1 - (16\eta/15)]$. Finally, the viscous pressure loss $\Delta p_v = 12\mu_p L U_p/\beta_p \bar{h}_p^2$, where L is the plug length. To ensure that velocity $\bar{u}(\bar{y},\bar{z})$ satisfies the no-slip condition at the side walls $\bar{y} = \pm 1/2$, a factor $\beta_p = 1 - 0.63a_p$ is included, similar to that reported elsewhere.[22]

Now, by equating the driving pressure ΔP_d with viscous pressure drop ΔP_v and using the deflection of the membrane at the trailing meniscus $\delta = h_p \eta$ and leading meniscus $\tilde{\delta}_p = h_p \eta_p$, we get

$$\left(\frac{\cos\theta_{pl}}{1-\eta_p} - \frac{1}{1-\eta}\right) = \frac{6\tilde{L}Ca}{\beta_p\left(1 - \frac{16\eta}{15}\right)^2}, \tag{6}$$

where $\tilde{L} = L/h_p$ is the non-dimensional plug length. The above equation is solved numerically in MATLAB to predict the capillary number Ca and thus the velocity of the plug U_p.

The dynamics of the DL meniscus is obtained by considering the increase in the driving pressure due to the decrease in the radius of curvature of the meniscus owing to the membrane deflection and the corresponding increase in the viscous pressure drop due to the decrease in the flow cross-sectional area. Before the DL meniscus interacts with the plug, the position of the DL meniscus $\tilde{x}_d$ as a function of time t is expressed as $\tilde{x}_d(t) = W_f\sqrt{t}$, where W_f is the modified Washburn coefficient W_f. For the DL channel, we have $\delta_d(x) = -\alpha p_d(x) w^4/D$. By differentiating, we get $-\frac{dp_d}{dx} = \frac{Dh_d}{\alpha w^4}\frac{d\eta_d}{dx}$, for $0 \le x \le \hat{x}_d$ in (Fig. 1(d)). Similar to the plug, we analyze the fully developed flow inside the DL to arrive at an equation similar to Equation (5). Using $\int\int d\bar{y}\, d\bar{z}\ \hat{u}_d(\bar{y},\bar{z}) = 1$, the hydraulic resistance per unit length of the deformed cross-section $R_d = \frac{1}{Q_d}\left(-\frac{\partial p_d}{\partial x}\right) = \frac{12\mu_d}{\beta w h_d^3}\frac{1}{F(\eta_d)}$, with $f(\eta_d) = 1 - (8/5)\eta_d + (128/105)\eta_d^2 - (1024/3003)\eta_d^3$, we rearrange to get $-\frac{dp_d}{dx} = R_d Q_d(t) = \frac{12\mu_d}{\beta_d w h_d^3}\frac{Q_d(t)}{f(\eta_d)}$, where $Q_d(t)$ is the instantaneous flow rate and $\beta_d = 1 - 0.63(h_d/w)$. By equating the two expressions for $-\frac{dp_d}{dx}$ and integrating from $x = 0$ to $\hat{x}_d$, we get

$$\frac{12\alpha\mu_d w^3}{\beta_d D h_d^4} Q_d(t)\,\hat{x}_d(t) = F(\hat{\eta}_d), \text{ where}$$
$$F(\hat{\eta}_d) = \hat{\eta}_d\left(1 - \frac{4\hat{\eta}_d}{5} + \frac{128\hat{\eta}_d^2}{315} - \frac{256\hat{\eta}_d^3}{3003}\right). \quad (7)$$

Assuming that the inertial effects[23] are negligible, we use $Q_d(t) \approx w h_d \frac{d}{dt}\hat{x}_d(t)\int\int 1\, d\bar{y}\, d\bar{z}|_{x=\tilde{x}_d}$ to get $\hat{x}_d\frac{d\hat{x}_d}{dt} = \frac{W_f^2}{2}$, where the modified Washburn coefficient W_f for the DL channel is

$$W_f = \sqrt{\frac{\beta_d F(\hat{\eta}_d) D h_d^3}{6\alpha A(\hat{\eta}_d)\mu_d w^4}}, \quad \text{where} \quad A(\hat{\eta}_d) = 1 - (4/15)\hat{\eta}_d. \quad (8)$$

When the DL meniscus approaches the trailing meniscus of the plug, owing to the pre-existing upward membrane deflection, there is a modification in the DL meniscus curvature and hence the corresponding driving pressure and velocity. The modified maximum deflection of the membrane $\hat{\delta}_{dp}$ (or $\hat{\eta}_{dp} = \hat{\delta}_{dp}/h_d$) is found by equating the driving pressure (approximated as the pressure at the DL meniscus) and the pressure causing the membrane deflection at this point as $\hat{\eta}_{dp} \approx 2\sigma_d\alpha\cos\theta_d w^4/(Dh_d^2(1 + h_p\eta/h_d)$. Thus, the modified reduced channel cross-sectional area at the meniscus is obtained as $A(\hat{\eta}_{dp}) = w h_d(1 + 8\hat{\eta}_d/15)$. The modified Washburn coefficient, which represents the velocity of the DL meniscus, while it crosses the plug is approximated as

$$W_{fp} = \sqrt{\frac{\beta_d F(\hat{\eta}_{dp}) D h_d^3}{6\alpha A(\hat{\eta}_{dp})\mu_d w^4}}. \quad (9)$$

Once the DL crosses the plug, the driving pressure increases again due to decrease in the channel cross-section. Since the length of the plug is small, once the DL overtakes the plug, the effect of the plug on the DL flow is negligible.

The devices were fabricated[24] by bonding two identical PDMS microchannels with width of 1100 μm and height of 160 μm with a thin PDMS membrane[12] with different thicknesses of 60–180 μm sandwiched in between the two microchannels (Fig. 1(e)). The device was mounted on a microscope stage (Axio Vert A1, Zeiss). First, a plug is created inside the upper microchannel by introducing 2 μl of liquid into the channel and then removing the excess liquid.[20] A DL drop of 0.1 ml is introduced into the adjoining microchannel, which fills the lower channel due to elastocapillary. The motion of the meniscus of the DL and plug are recorded using high-speed camera (FASTCAM SA3, Photron). The distance travelled by the plug and DL meniscus with time measured from experiments and predicted by model show good agreement within 11% (Fig. 2).The location of the plug with time was predicted from the velocity using Equation (6). The distance travelled by the DL meniscus was predicted using Equations (8) and (9), respectively, before and after the DL meniscus approaches the plug. The ratio of viscous force to capillary force is of the order of 1 even after a short distance of ~1.0 mm from the driving capillary flow inlet. Hence, inertia effects[23] are negligible and the use of Washburn model is justified. The error in position and time measurements were ±0.125 mm and ±0.004 s, respectively. Figs. 3(a) and 3(b) show the effect of J and plug length $\tilde{L}$ on plug velocity (or Ca) from the experiments and model, respectively. As J increases, the capillary force becomes stronger as compared with the restoring force due to which the driving differential pressure across the plug increases, which gives rise to higher plug velocity. While the model predicts a continuous increase in the velocity with the increase in J, for $J > 0.28$, a sudden decrease in velocity was observed in experiments. For higher J, the elastocapillary force is so strong that the initial upward deflection of the membrane is significant. The DL meniscus, when approaches the plug, experiences a diverging channel (neglected in the model) due to which the pressure jump across its meniscus is reduced significantly and thus the DL has negligible effect on the plug. In Fig. 3(b), the decrease in the plug velocity with the increase in the plug length is attributed to the higher viscous resistance offered by longer plugs. In Fig. 3(a), the maximum difference between the model predictions and experimental data is found to be <15% up to $J = 0.28$ (i.e., before side wall-wetting becomes predominant). A good match (error < 10%) is observed at lower values of J but at

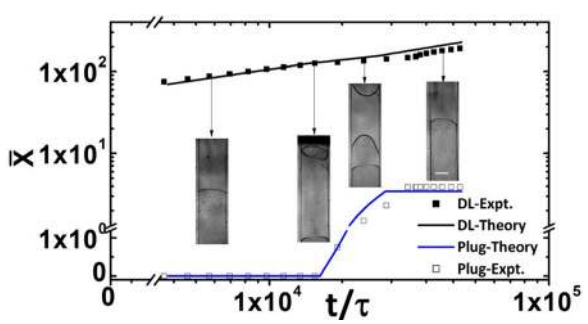

FIG. 2. Distance travelled by the menisci $\bar{X} = x/h_d$ of the DL (mineral oil) and the liquid plug leading end (olive oil) with time $t/\tau = t/\sqrt{\sigma\cos\theta/3\mu h_d}$, $\tilde{L} = 18.75$, size of channels is 1100 × 160 μm.

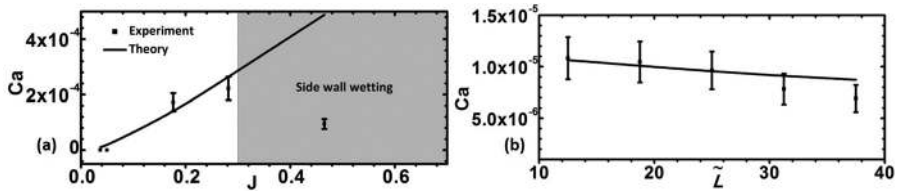

FIG. 3. Effects of (a) J, $\tilde{L}=31.25$ and (b) $\tilde{L}$, $J=0.05$, on plug velocity (Ca), in both cases, DL is silicone oil and size of channels is $1100\times160\,\mu$m.

higher J values (i.e., $J>0.28$), the error increases due to large initial upward deflection of the membrane, which is not accounted for in our model. Similarly, in Fig. 3(b), the match between the model and experiment is good (error $<10\%$) for shorter plugs, i.e., up to $\tilde{L}=31.25$. However, for longer plugs ($\tilde{L}>31.25$), the error is as high as 20%. This could be because, for longer plugs, the meniscus takes much longer time to completely cross the plug and therefore the reduction in pressure difference across the membrane at the trailing meniscus of the plug is more apparent, which is not addressed in our model. Thus, our model is accurate for lower range of J and $\tilde{L}$ values. In order to reduce the error at higher values of J and $\tilde{L}$, an improved 3D model is required. However, development of such a 3D model is extremely challenging and left as a future scope of the work.

Depending on the value of J, important flow regimes are observed. For $J<0.04$, due to large restoring force as compared with capillary force, the DL is unable to transport the plug. The membrane deflection is negligible and DL meniscus traverse through a rectangular channel and with its meniscus shape unchanged. For $0.40>J>0.04$, the DL is able to transport the plug (over $\delta_m\sim0.5$ mm for $J=0.13$), shown in Fig. 4(a), at various time instants (i-iii). According to Equation (2), the initial membrane deflection varies in y-direction (i.e., across width) as $\omega(x,y)=\delta_p(x)\left(4\left(\frac{y}{w}\right)^2-1\right)^2$. Due to the pre-existing deflection of the membrane, the DL meniscus, while crossing the trailing interface of the plug, experiences a diverging channel of height $h=h_d+16\delta_p(x)\left(\left(\frac{y}{w}\right)^2-\frac{1}{4}\right)^2$. By approximating the radius of curvature in the x-z plane $R_y=(h/2\cos\theta)$, the Laplace pressure jump across any point along the DL meniscus is obtained as

$$\Delta P=\sigma\left(\frac{1}{R_y}+\frac{1}{R_z}\right)=\sigma\left(\frac{2\cos\theta}{h_d+16\delta_p(x)\left(\left(\frac{y}{w}\right)^2-\frac{1}{4}\right)^2}+\frac{1}{R_z}\right),\tag{10}$$

where R_y and R_z are the first and second radii of curvature of the DL meniscus, respectively. The radius of curvature R_z of the DL meniscus is in the x-y plane. Similar expression for the pressure drop across a liquid meniscus inside a flexible nanochannels has been reported by van Honschoten *et al.*[25] Also, this pressure drop is fixed throughout the liquid meniscus as reported by Tas *et al.*[20] The deflected channel height increases from h_p at the sidewalls to $h_p+\delta_u(x)$ at the centre ($y=0$). Thus, $R_y=\left(h_p+16\delta_u(x)\left(\left(\frac{y}{w}\right)^2-\frac{1}{4}\right)^2\right)\Big/2\cos\theta$ continuously increases along the meniscus from the walls towards the centre. In order to maintain the same pressure jump ΔP at every point along the meniscus,[20] the R_z decreases from R_l to R_s at the centre of the channel (Figs. 4(a) and 4(b)). For $J>0.4$ (Fig. 4(b)), the R_z of the DL meniscus decreases at the centre but near to the wall, it increases rapidly to wet the walls completely. The DL meniscus at the centre moves very slowly or stops but near the walls it attains a large curvature and continues to move by completely wetting the walls. When the advancing DL meniscus near the walls arrives at the leading end of the plug, the shape of the plug meniscus is modified. This significantly improves the distance through which the leading meniscus of the plug is transported ($\delta_m>20$ mm, in Fig. 4(b)). When the DL meniscus arrives at the leading meniscus of the plug, the membrane is pulled towards the DL side. Thus, R_y of the leading meniscus of the plug increases over a region closer to the side walls. In order to maintain a constant pressure jump at every point along the leading meniscus of the plug, at the centre, the meniscus attains a negative radius of curvature R_z.

In conclusion, we presented a technique for the manipulation of a liquid plug inside a microchannel with a deformable wall. Theoretical model is developed, which predicts the plug velocity as a function of the non-dimensional parameter J and the plug length $\tilde{L}$. Self-powered transport of liquid plug has significance in various physical systems reported in the literature. The proposed technique could be used for coating chemicals inside microchannels,[19] controlled delivery of reagents and chemicals[28] inside microfluidic devices, and in a trigger valve system in a microfluidic device with the plug acting as the trigger.[8,9] Also, the proposed work could motivate in furthering the research on the interaction between fluid interfaces across soft membranes in microfluidic networks.[26,27]

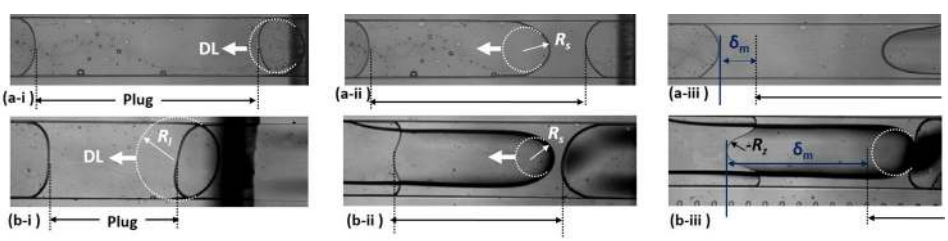

FIG. 4. Flow regimes. (a) $0.40>J>0.04$, the DL is able to transport the plug by some distance ($\delta_m\sim0.5$ mm for $J=0.13$) before crossing the liquid plug, DL undergoes a change in the meniscus shape. (b) $J>0.4$, DL wets sidewalls and causes a change in the meniscus shape at the leading end of the plug, plug moves by $\delta_m>20$ mm.

This work was supported by Indian Institute of Technology Madras via Project No. ERP 1314018 RESFASHS.

[1]G. M. Whitesides, Nature **442**, 368 (2006).
[2]E. W. Washburn, Phys. Rev. **17**, 273 (1921).
[3]J. W. van Honschoten, N. Brunets, and N. R. Tas, Chem. Soc. Rev. **39**, 1096 (2010).
[4]W. B. Young, Colloids Surf., A **234**, 123 (2004).
[5]Y. Zhu and K. Petkovic-Duran, Microfluid. Nanofluid. **8**, 275 (2010).
[6]V. Srinivasan, S. Khandekar, N. Bouamrane, F. Lefevre, and J. Bonjour, Exp. Fluids **56**(14), 1–6 (2015).
[7]M. Zimmermann, H. Schmid, P. Hunziker, and E. Delamarche, Lab Chip **7**, 119 (2007).
[8]M. Zimmermann, P. Hunziker, and E. Delamarche, Microfluid. Nanofluid. **5**, 395 (2008).
[9]R. Safavieh and D. Juncker, Lab Chip **13**, 4180 (2013).
[10]C. Py, P. Reverdy, L. Doppler, J. Bico, B. Roman, and C. N. Baroud, Phys. Rev. Lett. **98**, 156103 (2007).
[11]J. W. van Honschoten, M. Escalante, N. R. Tas, H. V. Jansen, and M. Elwenspoek, J. Appl. Phys. **101**, 094310 (2007).
[12]R. Anoop and A. K. Sen, Phys. Rev. E **92**, 013024 (2015).
[13]H.-Y. Kim and L. Mahadevan, J. Fluid Mech. **548**, 141 (2006).
[14]C. Duprat, J. M. Aristoff, and H. A. Stone, J. Fluid Mech. **679**, 641–654 (2010).
[15]Y. Zheng, H. Fujioka, S. Bian, Y. Torisawa, D. Huh, S. Takayama, and B. J. Grotberg, Phys. Fluids **21**, 071903 (2009).
[16]Y. D. Ma, Microfluid. Nanofluid. **12**, 671 (2012).
[17]M. Prakash, D. Quéré, and J. W. M. Bush, Science **320**, 931 (2008).
[18]P. Renvoisé, J. W. M. Bush, M. Prakash, and D. Quéré, Europhys. Lett. **87**, 39901 (2009).
[19]J. Bico and D. Quéré, J. Fluid Mech. **467**, 101 (2002).
[20]N. R. Tas, P. Mela, T. Kramer, J. W. Berenschot, and A. Van Den Berg, Nano Lett. **3**, 1537 (2003).
[21]M. Bracke, F. De Voeght, and P. Joos, Trends Colloid Interface Sci. III **79**, 142 (1989).
[22]H. Bruus, *Theoretical Microfluidics* (Oxford University Press, Inc., Oxford, 2008).
[23]S. Das, P. R. Waghmare, and S. K. Mitra, Phys. Rev. E **86**, 067301 (2012).
[24]P. Sajeesh, M. Doble, and A. K. Sen, Biomicrofluidics **8**, 054112 (2014).
[25]J. W. van Honschoten, M. Escalante, N. R. Tas, and M. Elwenspoek, J. Colloid Interface Sci. **329**, 133 (2009).
[26]S. Neukirch, B. Roman, B. de Gaudemaris, and J. Bico, J. Mech. Phys. Solids **55**, 1212 (2007).
[27]A. E. Cohen and L. Mahadevan, Proc. Natl. Acad. Sci. U. S. A. **100**, 12141 (2003).
[28]F. Sassa, J. Fukuda, and H. Suzuki, Anal. Chem. **80**, 6206 (2008).